AFTAC

Air Force Technical Applications Center

Directorate of Nuclear Treaty Monitoring

Theoretical Analysis of Narrow-Band Surface Wave Magnitudes

David R. Russell

30 June 2004

20041221 284
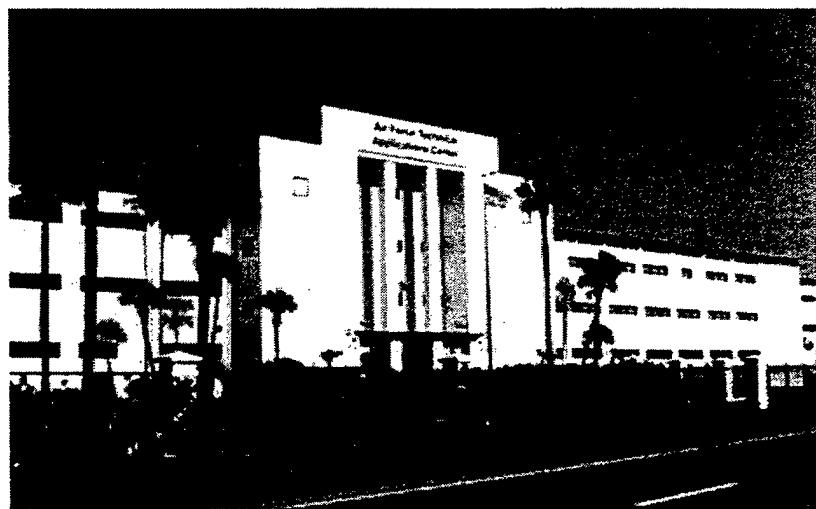
Report AFTAC-TR-04-004 has been reviewed and is approved for publication.

DAVID R, RUSSELL, SES
Director, Nuclear Treaty Monitoring
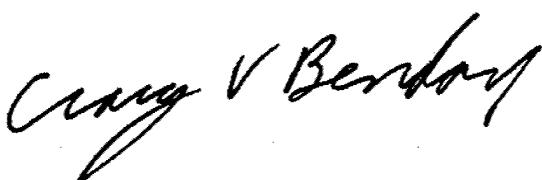
CRAIG V. BENDORF, Colonel, USAF
Commander

REPORT DOCUMENTATION PAGE		*Form Approved* *OMB No. 0704-0188*

Public reporting burden for this collection of information is estimated to average 1 hour per response, including the time for reviewing instructions, searching existing data sources, gathering and maintaining the data needed, and completing and reviewing this collection of information. Send comments regarding this burden estimate or any other aspect of this collection of information, including suggestions for reducing this burden to Department of Defense, Washington Headquarters Services, Directorate for Information Operations and Reports (0704-0188), 1215 Jefferson Davis Highway, Suite 1204, Arlington, VA 22202-4302. Respondents should be aware that notwithstanding any other provision of law, no person shall be subject to any penalty for failing to comply with a collection of information if it does not display a currently valid OMB control number. **PLEASE DO NOT RETURN YOUR FORM TO THE ABOVE ADDRESS.**

1. REPORT DATE *(DD-MM-YYYY)* 30 June 2004	2. REPORT TYPE Technical		3. DATES COVERED *(From - To)*
4. TITLE AND SUBTITLE Theoretical Analysis of Narrow-Band Surface Wave Magnitudes			**5a. CONTRACT NUMBER**
			5b. GRANT NUMBER
			5c. PROGRAM ELEMENT NUMBER
6. AUTHORS David R. Russell			**5d. PROJECT NUMBER**
			5e. TASK NUMBER
			5f. WORK UNIT NUMBER
7. PERFORMING ORGANIZATION NAME(S) AND ADDRESS(ES) Air Force Technical Applications Center (AFTAC/TT) 1030 S. Highway A1A Patrick AFB FL 32925-3002			**8. PERFORMING ORGANIZATION REPORT NUMBER** AFTAC-TR-04-004
9. SPONSORING/MONITORING AGENCY			**10. SPONSOR/MONITOR'S ACRONYM(S)**
			11. SPONSOR/MONITOR'S REPORT NUMBERS

12. DISTRIBUTION/AVAILABILITY STATEMENT

Approved for Public Release; Distribution Unlimited.

13. SUPPLEMENTARY NOTES

14. ABSTRACT

A major problem with time domain measurements of seismic surface waves is the significant effect of non-dispersed Rayleigh waves (Airy phases) which can occur at both regional and teleseismic distances. This paper derives a time domain method for measuring surface waves with minimum digital processing, using zero-phase Butterworth filters. This method can effectively measure surface wave magnitudes at both regional and teleseismic distances, while ensuring that the magnitudes are unbiased with respect to accepted formulae at reference periods, thus providing historical continuity. For applications over typical continental crust, the proposed magnitude equation is:

$$M_{S(b)} = \log(a_b) + \frac{1}{2}\log(\sin(\Delta)) + 0.0031\left(\frac{20}{T}\right)^{2.3}\Delta - 0.66\log\left(\frac{20}{T}\right) - \log(f_c) - 0.43$$

where a_b = measured filtered amplitude, T = period, and f_c = Butterworth filter corner frequency.

15. SUBJECT TERMS

surface waves   Butterworth filters   magnitudes   narrow-band   discrimination

16. SECURITY CLASSIFICATION OF:			17. LIMITATION OF ABSTRACT	18. NUMBER OF PAGES	19a. NAME OF RESPONSIBLE PERSON David R. Russell
a. REPORT UNCLASS	b. ABSTRACT UNCLASS	c. THIS PAGE UNCLASS	SAR	42	19b. TELEPHONE NUMBER *(include area code)* (321) 494-2356

Standard Form 298 (Rev 8-98)
Prescribed by ANSI Std. 239-18

(This page intentionally left blank.)

Contents

Figures

Tables

Acknowledgements

Theoretical Analysis
of
Narrow-Band Surface Wave Magnitudes

1. Introduction

Surface wave magnitudes are an indispensable tool for discriminating between shallow earthquakes and explosions, at least down to body wave magnitude $m_b = 4.0$. Seismologists have exhaustively studied surface wave magnitudes for years (e.g., Gutenburg, 1945; Vaněk et al., 1962; von Seggern, 1977; Okal, 1989; Rezapour and Pearce, 1998; and many others). However, operational methodologies for measuring surface waves still rely primarily on measuring unfiltered dispersed surface waves in the time domain, primarily in the vicinity of 20-second periods. A major problem with this approach is the significant effect of non-dispersed Rayleigh waves (Airy phases) which can occur at both regional and teleseismic distances, and can occur with dominant periods much less than 20 seconds. Errors introduced by measuring Airy phase signals can be greater than 0.5 magnitude units, or greater than a factor of three, which is unacceptable for reliable network averaging. Methods have been developed (Marshall and Basham, 1972) which apply empirical corrections based on geological regions for signals less than 20 seconds, but this only partially addresses the Airy phase problem.

With digital processing now widely available, we can optimize time domain processing and make possible automated routine measurements at variable periods. This paper investigates the use of narrow-band Butterworth filters for measuring surface waves, implemented as simple time domain digital filters, and pays attention to the effect of filtering on amplitudes and dispersion. The starting point is Herrmann (1973), who examined in detail theoretical surface wave envelope functions derived from rectangular and Gaussian frequency domain filters, and Yacoub (1983), who applied this methodology to automating surface wave measurements between 17-23 seconds, using narrow-band Gaussian filters. I also demonstrate how to modify currently accepted surface wave magnitude formulae to be unbiased with respect to narrow-band filtering at variable periods.

The first portion of the paper focuses on transformations of narrow-band Butterworth filters operating on dispersed waveforms from the frequency domain to the time domain, without incorporating geometric spreading and attenuation effects. Asymptotic formulae are evaluated for simple frequency/time transformations, with corresponding error analysis.

The second part of the paper reviews surface wave magnitudes from a theoretical point of view, by correcting frequency domain amplitudes for dispersion, geometric spreading, and attenuation, and showing how this results in currently accepted magnitude corrections. Using the results of the first part, narrow-band Butterworth measurements are incorporated into accepted magnitude corrections, resulting in a new formula which is unbiased with respect to 20-second measurements, at variable periods between 5-25 seconds.

2. Surface Wave Amplitudes

A filtered, dispersed propagating surface wave normal mode can be expressed as (Herrmann, 1973):

$$a(t,x) = \frac{1}{2\pi} \int_{-\infty}^{\infty} H(\omega) A(\omega) e^{i(\omega t - k(\omega)x)} d\omega \qquad (1)$$

where ω is the angular frequency, $H(\omega)$ is a band-pass filter symmetric about center frequency ω_0, $A(\omega)$ is the complex amplitude of the normal mode, and $k(\omega)$ is the wavenumber. $A(\omega)$ is also distance dependent if geometric spreading and attenuation are considered. These corrections will be ignored for now to concentrate on the effects of dispersion, and discussed in detail in the section on surface wave magnitudes. To approximate the dispersive characteristics of the propagating wave, expand the phase as a Taylor series about a center frequency ω_0, ignoring higher order terms beyond the quadratic:

$$(\omega t - kx) = \phi_0 + \beta(\omega - \omega_0) - \alpha(\omega - \omega_0)^2 \qquad (2)$$

where (Herrmann, 1973; Aki and Richards, 1980)

$$\phi_0 = \omega_0 t - k_0 x, \quad \beta = t - x\frac{dk}{d\omega}\bigg|_0 = t - \frac{x}{U_0}, \quad \alpha = \frac{x}{2}\frac{d^2 k}{d\omega^2}\bigg|_0 = \frac{x}{4\pi}\frac{T_0^2}{U_0^2}\frac{dU}{dT}\bigg|_0 \qquad (3)$$

U is the group velocity and T is the period corresponding to the angular frequency ω. Following Papoulis (page 123, 1962) *we make the assumption that $H(\omega)$ is a narrow-band symmetric filter and $A(\omega)$ is approximately constant across the bandwidth of H.* Then, substituting (2) into (1) and making the variable substitution $\omega + \omega_0 \rightarrow \omega$ gives the following:

$$a(t,x) = A_0 e^{i\phi_0} \frac{1}{\pi} \int_{-\infty}^{\infty} H_L(\omega) e^{i(\beta\omega - \alpha\omega^2)} d\omega \qquad (4)$$

where $A_0 = A(\omega_0)$, and $H_L(\omega) = H(\omega + \omega_0)$ is an equivalent low-pass filter. The real part of the complex expression (4) is equivalent to (1). The envelope maximum corresponding to the group velocity $\beta = 0$ is defined as:

$$|a_0| = A_0 \frac{1}{\pi} \left| \int_{-\infty}^{\infty} H_L(\omega) e^{-i\alpha\omega^2} d\omega \right| \qquad (5)$$

This expression shows that, for a narrow-band process, the maximum time domain amplitude is equivalent to the frequency domain amplitude modulated by two low pass filters: H_L and

2

$e^{-i\alpha\omega^2}$. For values of ω away from the origin, the exponential integrand will rapidly oscillate, not contributing to the integral, and thus act as a low pass filter. As a result, the time domain amplitude can be controlled by either filter, depending on the value of the cutoff frequency ω_c, of H_L, or the value of α in the exponent. This can be seen graphically in Figure 1:
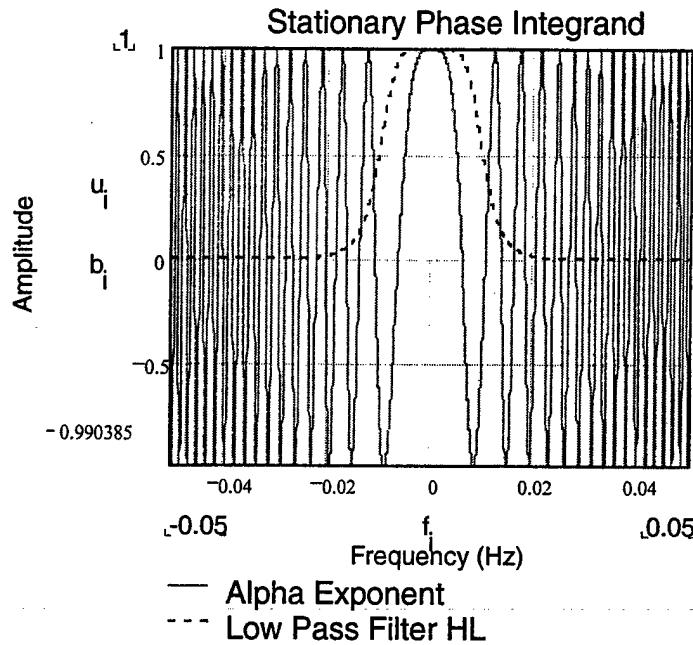
Figure 1.

As the value of α increases, the width of the fundamental lobe of the exponential integrand will decrease, thus controlling the bandwidth of the recorded amplitude. If the value of the bandwidth of H_L decreases below the exponential bandwidth, it will control the amplitude of the recorded signal. This trade-off can be useful in modifying the dispersion measured on observed seismograms, as will be discussed below.

3. Application of Butterworth Filters

As a specific case of the low-pass filter H_L, let us use a zero phase n[th] order Butterworth band-pass filter of the form (Kanasewich, 1975)

$$H(\omega) = \frac{1}{1 + \left(\dfrac{\omega - \omega_0}{\omega_c}\right)^{2n}} \qquad (6)$$

where $2\omega_c$ is the bandwidth about ω_0, defined at one-half the amplitude of $H(\omega)$. Then,

$$H_L(\omega) = \cfrac{1}{1+\left(\cfrac{\omega}{\omega_c}\right)^{2n}} = \cfrac{\omega_c^{2n}}{\omega^{2n}+\omega_c^{2n}} \tag{7}$$

Substituting (7) into (4) gives

$$a(t,x) = A_0 e^{i\phi_0} \frac{1}{\pi} \int\limits_{-\infty}^{\infty} \frac{\omega_c^{2n}}{\omega^{2n}+\omega_c^{2n}} e^{i(\beta\omega - \alpha\omega^2)} d\omega \tag{8}$$

Expanding H_L as partial fractions and using relationship 7.4.2 from Abromowitz and Stegun (1964), $a(t,x)$ can be shown to equal (see Appendix A):

$$a(t,x) = A_0 e^{i\phi_0} \frac{e^{i\frac{\beta^2}{4\alpha}}}{2n} \sum_{k=1}^{n} \varepsilon_k \left[e^{\Psi_k^2(+\beta)} erfc(\Psi_k(+\beta)) + e^{\Psi_k^2(-\beta)} erfc(\Psi_k(-\beta)) \right] \tag{9}$$

where $erfc$ is defined as the complementary error function ($1-erf$),

$$\Psi_k(\pm\beta) = e^{i\frac{\pi}{4}}\left(\sqrt{\alpha}\varepsilon_k \pm i\frac{\beta}{2\sqrt{\alpha}} \right) \tag{10}$$

$$\varepsilon_k = \omega_c e^{i\theta_k} \tag{11}$$

$$\theta_k = \frac{\pi(2k-n-1)}{2n} \tag{12}$$

and recalling from equation (3) that

$$\beta = t - \frac{x}{U_0}, \qquad \alpha = \frac{x}{4\pi} \frac{T_0^2}{U_0^2} \frac{dU}{dT}\bigg|_0 \tag{13}$$

As an example, set (typical for continental crusts)

$$X = 6000 \text{ km}, \quad T_0 = 20 \text{ sec}, \quad U_0 = 2.9 \text{ km/sec}, \quad \frac{dU}{dT}\bigg|_0 = .02 \text{ km/sec}^2 \tag{14}$$

Let the order of the Butterworth filter be $n = 3$, and the corner of the filter $f_c = .005$ Hertz. Substituting these values into equation (9) and plotting the real value as a function of β gives the seismogram illustrated in Figure 2.
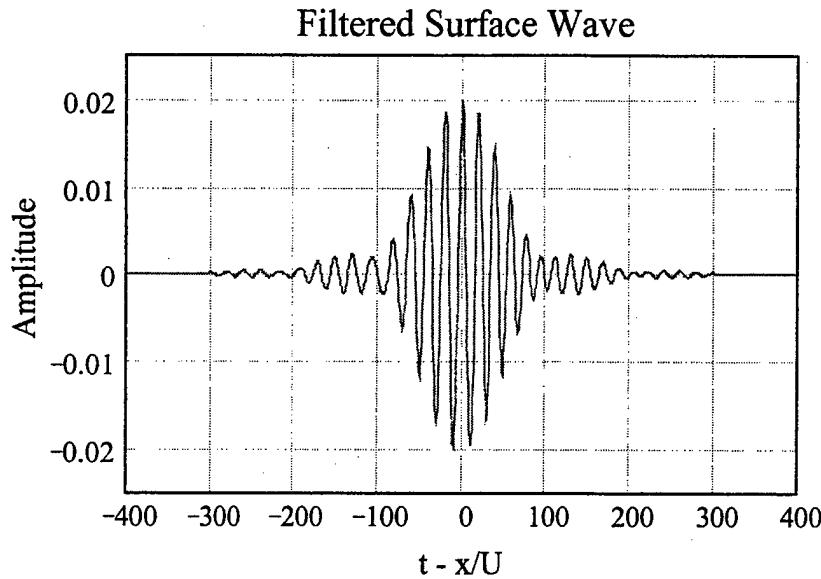
Figure 2.

Notice that the plot has a maximum at the group velocity $U_0 = x/t$.

4. Asymptotic Values of Filtered Amplitudes

At the amplitude maximum corresponding to the group velocity ($\beta = 0$), equation (9) reduces to:

$$a_0 = A_0 e^{i\phi_0} \frac{1}{n} \sum_{k=1}^{n} \varepsilon_k e^{i\alpha\varepsilon_k^2} erfc(\sqrt{i\alpha}\,\varepsilon_k) \tag{15}$$

where

$$\varepsilon_k = \omega_c e^{i\theta_k} \tag{16}$$

$$\theta_k = \frac{\pi(2k-n-1)}{2n} \tag{17}$$

For large ω_c or α, the following asymptotic form for *erfc* can be used (Abromowitz and Stegun, relation 7.1.23, 1964; Mathews and Walker, page 80, 1970):

$$erfc(u) \approx \frac{e^{-u^2}}{\sqrt{\pi}\,u} \tag{18}$$

5

Letting $u = \sqrt{i\alpha}\,\varepsilon_k$, and substituting (13) and (18) into (15) gives, after some algebraic manipulation,

$$|a_0| = \left|\frac{A_0}{\sqrt{\pi i \alpha}}\right| = 2\frac{A_0 U_0}{T_0 \sqrt{\left|\dfrac{dU}{dT}\right|}\,x} \tag{19}$$

This is precisely the value arrived at by Okal (1989) assuming strongly dispersed surface waves (α large). *Notice that equation (19) is independent of ω_c, thus independent of H_L.*

For small values of α in the exponential integrand, it is expected that the main lobe will be wide (Figure 1), so the amplitude will be controlled by the low-pass filter H_L. Letting $\alpha \to 0$ in equation (15) results in

$$a_0 = A_0 e^{i\phi_0} \frac{\omega_c}{n} \sum_{k=1}^{n} e^{i\theta_k} \tag{20}$$

which is controlled only by the order of the Butterworth filter H_L and its corner frequency ω_c. For a 3rd order filter ($n = 3$), and recalling equation (17), equation (20) immediately reduces to

$$|a_0| = A_0 \frac{2\omega_c}{3} \tag{21}$$

Figure 3 shows the envelope of equation (15) as a function of α, along with the asymptotic values (19) and (21), assuming a 3rd order Butterworth filter with a filter corner of $f_c = .005$ Hertz:

Max Amplitude v.s. Alpha

— Butterworth Filter
- - Small Alpha Asymptote
— - Large Alpha Asymptote
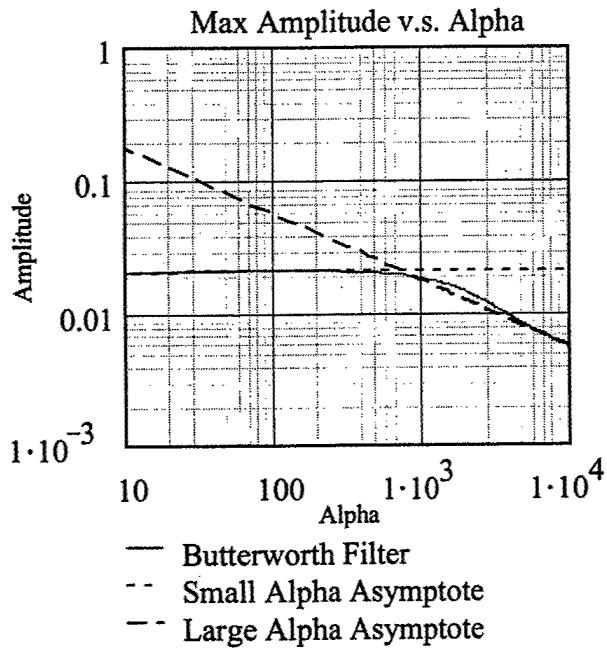
Figure 3.

Notice that the Butterworth filtered surface wave shows *almost constant amplitude (minimal dispersion)* out to a value of $\alpha \cong 800$, where the asymptotes intersect.

For any value of α, ω_c, and n, this can be generalized as follows: looking only at absolute values, rewrite (19) and (21) as

$$|a| = \frac{A_0}{\sqrt{\pi\alpha}} \qquad (22)$$

$$|a_b| = A_0\omega_c r_n \,, \qquad r_n = \frac{1}{n}\sum_{k=1}^{n} e^{i\theta_k} = \frac{1}{n}\sum_{k=1}^{n}\cos(\theta_k) \qquad (23)$$

Notice that the exponential term in r_n reduces to the cosine term due to the symmetric distribution of θ_k (see equation 17). Define the asymptotic intercept as the point where the equations are equal:

$$\omega_c r_n = \frac{1}{\sqrt{\pi\alpha}} \qquad (24)$$

Assuming minimal dispersion for values of α less than the intercept results in

$$\alpha \leq \frac{1}{\pi(\omega_c r_n)^2} $$

or equivalently,

$$\omega_c \leq \frac{1}{r_n\sqrt{\pi\alpha}} \qquad (25)$$

Equation (25) determines the range of cutoff frequencies for which a Butterworth filter can be constructed to reduce the dispersion error to a minimum.

To justify the assumption of minimal dispersion, the absolute error between the Butterworth amplitude and the asymptotic value at the intercept can be determined as follows. Evaluate and rearrange the Butterworth amplitude (15) at the intercept point (24) as:

$$a_{INT} = A_0\omega_c Z_n \qquad (26)$$

where

$$Z_n = \left|\frac{1}{n}\sum_{k=1}^{n} e^{i(V_k^2+\theta_k)}erfc(V_k)\right|, \qquad V_k = \frac{e^{i\theta_k}}{r_n\sqrt{\pi}} \qquad (27)$$

It can be seen by inspection that Z_n is *only* a function of the Butterworth order n.

Define the logarithmic error between the Butterworth amplitude and asymptote as:

$$ERR = LOG(ASYMPTOTE) - LOG(AMPLITUDE)$$

Evaluate at the intercept using (23) and (26) for:

$$ERR = LOG(A_0 \omega_c r_n) - LOG(A_0 \omega_c Z_n)$$

or

$$ERR = LOG\left(\frac{r_n}{Z_n}\right) \tag{28}$$

Notice that the logarithmic error is only a function of the Butterworth order n. Table 1 gives the values of *ERR* for the first six Butterworth orders:

Table 1.
Butterworth Order vs. Log Error

n	1	2	3	4	5	6
ERR	0.191	0.0672	0.0360	0.0244	0.0193	0.0168

For Butterworth filters of order 3 (recommended) or greater, the maximum magnitude error will be less than or equal to 0.0360 for values of ω_c satisfying the inequality in (25).

5. Surface Wave Magnitudes

Surface wave magnitudes are generally expressed as distance-corrected logarithmic amplitude measurements of surface waves in the time domain, usually measured in the vicinity of 20-second vertical component Rayleigh waves. Typically, the amplitude measurements are corrected for instrument response to either zero-to-peak or peak-to-peak amplitude measurements, usually in millimicrons or nanometers. Time domain formulae for surface wave magnitudes are generally derived from empirical measurements of surface wave amplitudes averaged across many events and epicentral distances (e.g., Vaněk et al., 1962; von Seggern, 1977; Rezapour and Pearce, 1998).

Surface wave magnitudes can also be derived theoretically by correcting frequency domain amplitudes for geometric spreading and attenuation (Kanamori and Stewart, 1976) and then transforming to the time domain (Okal, 1989). Let

$$A_c = A\sqrt{r_e \sin(\Delta)} \, e^{\frac{\pi \kappa \Delta}{UQT}} \tag{29}$$

where

A_c = Corrected frequency domain amplitude
A = Frequency domain amplitude
r_e = Earth's radius
Δ = Epicentral distance in degrees
κ = Degree to kilometer conversion (111.2 km/deg)
T = Period of interest
Q = Q factor measuring attenuation at period T
U = Group velocity at period T

To transform (29) into the time domain, recall the strong dispersion relation for surface wave amplitudes (19) (see also Okal, 1989):

$$a = \frac{2U}{T\sqrt{\frac{dU}{dT}}\kappa\Delta} A \tag{30}$$

Solve (30) for A and substitute into (29) to arrive at a theoretical expression for corrected time domain amplitudes at frequency T:

$$a_c = aT\sqrt{r_e \sin(\Delta)}\, e^{\frac{\pi\kappa\Delta}{UQT}} \frac{\sqrt{\frac{dU}{dT}}\kappa\Delta}{2U} \tag{31}$$

Taking the base 10 logarithm of (31) results in an expression for surface wave magnitudes:

$$M_s = \log(aT) + \frac{1}{2}\log(\sin(\Delta)) + \log(e)\frac{\pi\kappa\Delta}{UQT} + \frac{1}{2}\log(\Delta) + \log\left(\sqrt{\frac{dU}{dT}}\Big/U\right) + C \tag{32}$$

where constants are now combined in C. The correction terms represent distance adjustments for geometric spreading, attenuation, and dispersion. The last term is a period-dependent dispersion correction. The undetermined constant C is determined from empirical time domain measurements.

Okal (1989) showed that the attenuation and dispersion terms in (32) are roughly proportional as follows *when evaluated in the vicinity of 20-second periods*:

$$B\log(\Delta) \propto \frac{1}{2}\log(\sin(\Delta)) + \log(e)\frac{\pi\kappa\Delta}{UQT} + \frac{1}{2}\log(\Delta) \tag{33}$$

and

$$\log(1/T^2) \propto \log(e)\frac{\pi\kappa\Delta}{UQT} + \log\left(\sqrt{\frac{dU}{dT}}\Big/U\right) \tag{34}$$

where B is a constant in (33). It should be noted that Okal also included a source excitation correction in (34). However, (34) is a very *rough* approximation, which depends strongly on the value of dU/dT. Notice that for Airy phases, $dU/dT \rightarrow 0$, which can cause *large* errors in the magnitude.

Substituting (33) and (34) into (32) results in the standard formulation for surface wave magnitudes (Vaněk et al., 1962; von Seggern, 1977):

$$M_s = \log(a/T) + B\log(\Delta) + C \tag{35}$$

or, if only (34) is used (von Seggern, 1977; Rezapour and Pearce, 1998):

$$M_s = \log(a/T) + \frac{1}{2}\log(\sin(\Delta)) + B_{att}\Delta + \frac{1}{2}\log(\Delta) + C \tag{36}$$

The term B_{att} in (36) is a constant defining the attenuation. It should be noted that Rezapour and Pearce prefer using a coefficient of 1/3 instead of 1/2 in the dispersion term of (36), in order to account for distance effects of Airy phase propagation.

5.1 Surface Wave Magnitudes from Narrow-band Butterworth Filters

The theoretical derivation of surface wave magnitudes for narrow-band filters is considerably simplified from the above, since the frequency to time-domain transformation is non-dispersive, for values of ω_c satisfying the inequality in (25). Recall the asymptotic value for an nth order Butterworth filter (equation 23):

$$a_b = \omega_c r_n A \tag{37}$$

where a_b is the filtered time domain Butterworth amplitude, and ω_c is the Butterworth corner frequency. Solving for A and substituting this expression into (29) gives the corrected Butterworth filtered time-domain amplitude at period T:

$$a_{bc} = \frac{a_b}{\omega_c r_n} \sqrt{r_e \sin(\Delta)} \, e^{\frac{\pi \kappa \Delta}{UQT}} \tag{38}$$

Taking logarithms of (38) results in the time-domain magnitude formula:

$$M_{s(b)} = \log(a_b) + \frac{1}{2}\log(\sin(\Delta)) + \log(e)\frac{\pi \kappa \Delta}{UQT} - \log(f_c) + C_b \tag{39}$$

where constants in (38) are now combined in C_b, and $\omega_c = 2\pi f_c$. Notice that the correction terms are now geometric spreading, attenuation, and the value of the Butterworth corner frequency.

From (39) the final formula for narrow-band filtering with a fixed attenuation coefficient can be written as

$$M_{s(b)} = \log(a_b) + \frac{1}{2}\log(\sin(\Delta)) + B_{att}\frac{T_0}{T}\Delta - \log(f_c) + C_b \tag{40}$$

where it is assumed that variations in the attenuation terms in (39) are small around the reference period T_0. The constants B_{att} and C_b in (40) can be found by empirically measuring surface wave amplitudes a_b across different epicentral distances Δ.

5.2 Normalizing Butterworth Magnitudes to Standard Magnitude Formulae

An alternative to determining the constants B_{att} and C_b empirically is to transform (40) into the standard formula (36) at reference period T_0, and then calculate the Butterworth constants based on standard formula constants. This has the advantage of ensuring that Butterworth magnitudes are unbiased with respect to currently accepted magnitudes, at least at given reference periods. To accomplish this, first recall the frequency to time transformations given in (22) and (23):

$$a = \frac{A}{\sqrt{\pi\alpha}}, \quad a_b = \omega_c r_n A \tag{41}$$

The first transformation represents surface wave amplitudes measured on essentially unfiltered and non-Airy-phase seismograms, and the second is the amplitude measured after Butterworth filtering with a corner frequency satisfying the inequality given in (25). Under these conditions the unfiltered time domain measurement can be transformed into the filtered measurement by equating frequency domain amplitudes in (41):

$$a_b = \left(\omega_c r_n \sqrt{\pi\alpha}\right)a \tag{42}$$

Recalling the definition of α in (3), equation (42) can be rewritten in terms of measured quantities as:

$$a_b = \frac{f_c T \sqrt{\Delta}}{G}a \tag{43}$$

where G is defined as:

$$G = \frac{U}{\pi r_n \sqrt{\frac{dU}{dT}\kappa}} \tag{44}$$

κ, Δ are defined as in (29), and $\omega_c = 2\pi f_c$. Also using (3), equation (25) can be rewritten as

11

$$f_c \leq \frac{G}{T\sqrt{\Delta}} \tag{45}$$

Notice that when the equality holds in (45), $a_b = a$ in (43).

Now, to do the transformation, assume that a large number of measurements have been made at a reference period T_0 on a *core seismic network*, which is distributed across given geographic areas, with source/receiver propagation paths representing an average type of geologic structure. Define the average group velocity at T_0 for this structure as U_0 and its derivative as $dU/dT|_0$. Define the corresponding value of G in (44) as G_0. Evaluating (43) at G_0 and T_0 and substituting into (40) gives

$$M_s = \log(aT_0) + \frac{1}{2}\log(\sin(\Delta)) + B_{att}\Delta + \frac{1}{2}\log(\Delta) + C_b - \log(G_0) \tag{46}$$

Adding and subtracting $\log(T_0^2)$ in (46) gives

$$M_s = \log(a/T_0) + \frac{1}{2}\log(\sin(\Delta)) + B_{att}\Delta + \frac{1}{2}\log(\Delta) + C_b - \log\left(\frac{G_0}{T_0^2}\right) \tag{47}$$

Equating (36) and (47) shows that the two equations are equal at the reference period T_0 if C_b is defined as

$$C_b = C + \log\frac{G_0}{T_0^2} \tag{48}$$

and B_{att} is equivalent for both equations. Thus, the Butterworth magnitude (40) can be derived to be unbiased with respect to standard magnitudes by defining G_0 and determining the constant C_b from (48).

Finally, it should be noted that the value of f_c bounded in (45) must be calculated from actual values of G, T, and Δ for individual measurements in order to minimize dispersion error for each measurement. However, since (45) is an inequality, if a minimum value G_{min} can be found for all expected propagation paths, this can be used to define f_c as

$$f_c \leq \frac{G_{min}}{T\sqrt{\Delta}} \tag{49}$$

and this will result in minimum dispersion error across the network for all propagation paths, given knowledge of T and Δ for individual events.

5.3 Butterworth Magnitude Formula at Variable Periods

It should be emphasized that the above derivation is only valid in the vicinity of 20-second periods. The above formula should not be extrapolated to short periods without correcting for period-dependent source excitation and attenuation. Typically, explosions and shallow

earthquakes have source excitation functions which increase by a factor of about 0.2 magnitude units from 20- to 10-second periods, and again by 0.2 magnitude units between 10- and 5-second periods. Also, numerous studies (e.g., Herrmann and Mitchell, 1975) have shown that the attenuation coefficient (km^{-1}) can increase by a factor of three or more from 10- to 5-second periods. Therefore, it is advisable to modify equation (40) with functions which adequately approximate this behavior, if unbiased short period magnitudes are required. However the functions are constructed, they should be normalized at $T_0 = 20$ seconds to reflect standard magnitude formulae.

Candidate functions can be constructed with the form T_0/T to normalize at T_0. To modify the attenuation coefficient, the following form is suggested:

$$B(T) = B_{att}\left(\frac{T_0}{T}\right)^{\gamma}$$

(50)

When $T = T_0$, the function reduces to the constant coefficient B_{att}. The value of the coefficient γ can be chosen to reflect the increase the value of the coefficient at shorter periods.

For the source excitation, the following function can be constructed to correct the magnitude formula for typical short period increases in source amplitude:

$$S(T) = -S_0 \log\left(\frac{T_0}{T}\right)$$

(51)

When $T = T_0$, the source function contributes no correction and, for other periods, the value S_0 controls the amount of correction at shorter periods.

With the above corrections, a final form of the Butterworth magnitude formula for variable periods can be expressed as follows:

$$M_{s(b)} = \log(a_b) + \frac{1}{2}\log(\sin(\Delta)) + B_{att}\left(\frac{T_0}{T}\right)^{\gamma}\Delta - S_0 \log\left(\frac{T_0}{T}\right) - \log(f_c) + C_b$$

(52)

$$f_c \leq \frac{G_{min}}{T\sqrt{\Delta}}$$

(53)

To calculate $M_{s(b)}$, the following steps should be taken:

- Determine the epicentral distance in degrees to the event Δ and the period T.

- Calculate the corner frequency f_c of the Butterworth filter from (53).

- Filter the time series with a zero-phase Butterworth band-pass filter with corner frequencies $1/T-f_c$, $1/T+f_c$.

- Calculate maximum amplitude a_b of filtered signal.

- Determine $M_{s(b)}$ from (52).

5.4 Specific Examples

Three commonly used formulae for surface wave magnitudes (amplitudes measured zero-to-peak, in millimicrons) are given by

Prague (Vaněk et al., 1962):

$$M_s = \log(a/T) + 1.66\log(\Delta) + 0.3 \tag{54}$$

Von Seggern - normalized to Prague at 50 degrees (von Seggern, 1977):

$$M_s = \log(a/T) + \frac{1}{2}\log(\sin(\Delta)) + 0.0031\Delta + \frac{1}{2}\log(\Delta) + 2.2 \tag{55}$$

Rezapour and Pearce (Rezapour and Pearce, 1998):

$$M_s = \log(a/T) + \frac{1}{2}\log(\sin(\Delta)) + 0.0046\Delta + \frac{1}{3}\log(\Delta) + 2.37 \tag{56}$$

Plotting the magnitude corrections as a function of epicentral distance gives:
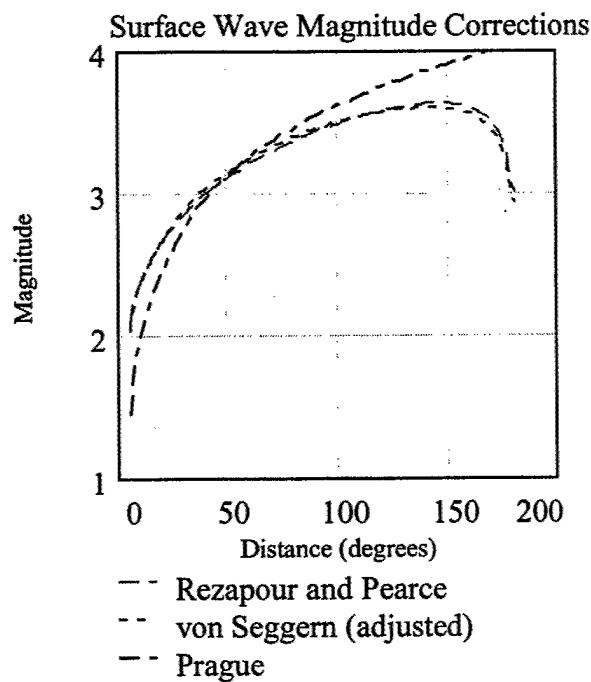
Figure 4.

As can be seen from the figure, the Rezapour and Pearce correction is almost identical to the von Seggern correction. Although the Prague formula biases magnitude corrections to oceanic propagation paths, it is still used to normalize newer formulae to maintain historical continuity. For purposes of this study, the von Seggern formula will be used as a baseline, where $B_{att} = 0.0031$, and $C = 2.2$.

To calculate the normalized Butterworth magnitude equation, assume a network defined primarily over continental paths, and measured at the reference period 20 seconds. Let:

$$
\begin{aligned}
T_0 &= 20 \text{ sec} \\
U_0 &= 2.9 \text{ km/sec} \\
(dU/dT)_0 &= 0.02 \text{ km/sec}^2
\end{aligned}
$$

Also assume a 3rd order Butterworth filter. From equations (17) and (23):

$$
r_n = \sum_{k=1}^{3} \cos(\theta_k) = \frac{2}{3}
$$

Using the above values, and equations (44) and (48):

$$
G_0 = 0.93, \quad C_b = -0.43
$$

To determine G_{min}, use equation (44), and look at values of T, U, and dU/dT that minimize G for various paths and periods in the core network. Setting $G_{min} = 0.6$ should cover continental signals between 8 and 40 seconds, and oceanic signals between 20 and 40 seconds, including mixed oceanic and continental. This assumes a 20-second oceanic group velocity of $U = 3.6$ km/sec and derivative $dU/dT = .08$ km/sec^2. *The value of G_{min} should be lowered down to 0.2 or less for deep sediment structures at periods between 5 and 8 seconds, and short period oceanic paths between 5 and 20 seconds.*

To determine the period dependent attenuation coefficient, use the form given by (50) and, from von Seggern, use $B_{att} = 0.0031$ (0.278 x 10^{-4} km^{-1}). To find γ, find the best fit of equation (50) to empirical continental attenuation coefficient data. For instance, Herrman and Mitchell (1975) published values of anelastic attenuation for the stable interior of North America for both shallow earthquakes and nuclear explosions. Plotting the values for Rayleigh wave attenuation with $\gamma = 2.3$ gives:
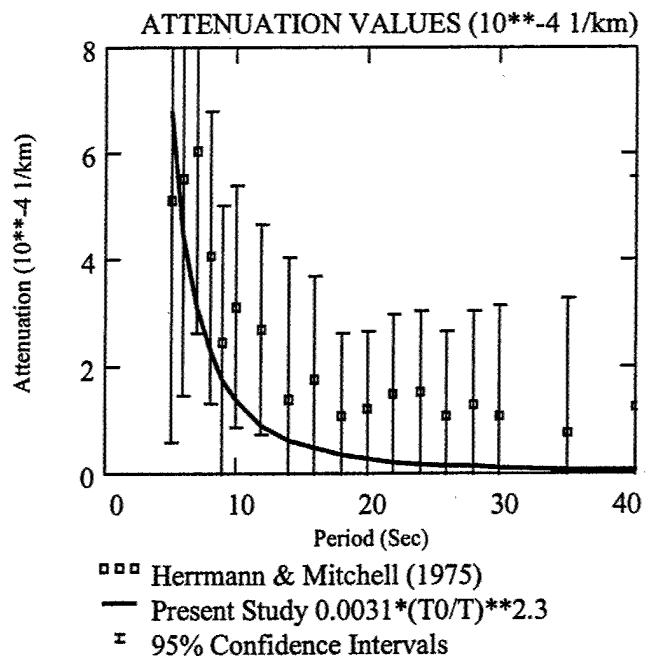
Figure 5.

Notice that the value of $B(T)$ in the present study is lower than suggested by Herrmann and Mitchell; this is due to forcing the function to fit $B_{att} = 0.0031$ (0.278×10^{-4} km^{-1}) at 20 seconds. The point is to ensure that $B(T)$ adequately reflects the significant increase in attenuation over continental paths at short periods.

To determine the correction for source excitation, use equation (51) and assume the source to be a shallow earthquake or explosion. In this case, there should be an increase in amplitude between 20 and 10 seconds by approximately 0.2 magnitude units, with the same increase between 10 and 5 seconds. A value of $S_0 = 0.66$ will correct for this excitation as shown in Figure 6:

Source Amplitude Correction

Correction: -0.66*log(T0/T)
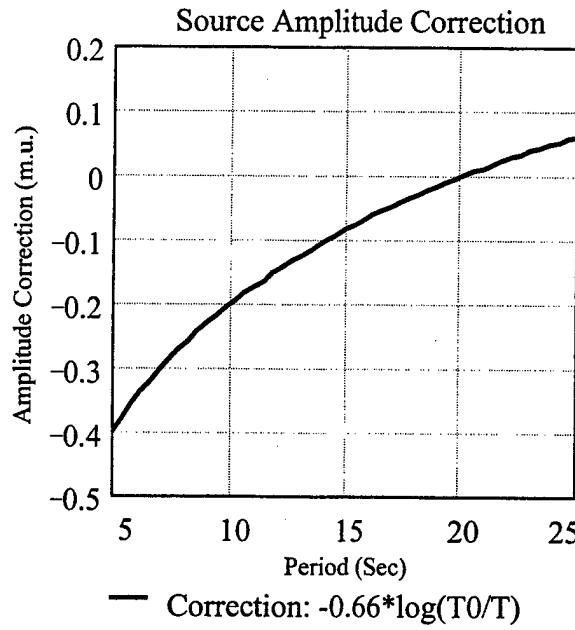
Figure 6.

Combining all of the above into (52) and (53) results in the Butterworth magnitude formula:

$$M_{s(b)} = \log(a_b) + \frac{1}{2}\log(\sin(\Delta)) + 0.0031\left(\frac{20}{T}\right)^{2.3}\Delta - 0.66\log\left(\frac{20}{T}\right) - \log(f_c) - 0.43 \qquad (57)$$

$$f_c \le \frac{0.6}{T\sqrt{\Delta}} \qquad (58)$$

Again, it should be noted that a value of $G_{min} = 0.6$ should be valid for most continental paths with $8 \le T \le 25$ seconds, and oceanic paths with $T > 20$ seconds. For paths in deep sediments with $5 \le T \le 8$ seconds, and oceanic paths with $5 \le T \le 20$ seconds, a value of $G_{min} = 0.2$ should be more appropriate to reflect the strong dispersion present. Also note that the use of this formula will fully correct measurement errors due to Airy phases.

6. Summary

In summary, the above theory gives a method to calculate surface wave magnitudes over broad period and distance intervals. The fundamental goals of the study were to develop a surface wave methodology which can:

- Measure signals in the *time domain* with minimum digital processing using Butterworth filters.

- Effectively measure unbiased surface wave magnitudes at both regional and teleseismic distances, while being applicable across a wide range of periods.

- Ensure that the formula is unbiased with respect to accepted formulae at reference periods, providing historical continuity.

With rough estimates of group velocity and derivative bounds, the formula is unbiased with respect to standard 20-second historical M_s measurements, down to 5-second periods and distances of less than 200 km. The strength of the method is that it solves the problem of trying to simultaneously measure *in the time domain* well-dispersed surface waves at teleseismic distances with non-dispersed or Airy phases at regional distances. The weakness of the methodology at this point is the analysis of attenuation. Although the above formula (equation 50) compensates for attenuation down to 5 seconds on continental structures, it is clearly oversimplified for both regional and teleseismic distances and is the largest remaining source of error for surface wave magnitudes. More study is needed to define regionally varying propagation paths, including oceanic, deep sediments, and basin and range structures, with emphasis on analyzing variability between 5-25 seconds across these paths. To account for regionally varying attenuation, the theoretical attenuation term in (39) can be regionalized as:

$$\frac{\log(e)\pi\kappa}{UQT}\Delta \to B_{ij}(T)\Delta \tag{59}$$

where

$$B_{ij}(T) = \frac{\log(e)\pi\kappa}{U(T)Q_{ij}(T)T} \tag{60}$$

In (60), both $U(T)$ and T can be determined directly from individual narrow-band filtered seismograms; however, what must be understood is the variability of Q over multiple source/receiver paths ij at different periods T.

Appendix A

Derivation of Filtered Surface Wave Integral

The purpose of this appendix is to derive the solution to the integral

$$I_n = \frac{1}{\pi} \int_{-\infty}^{\infty} \frac{\omega_c^{2n}}{\omega^{2n} + \omega_c^{2n}} \, e^{i(\beta\omega - \alpha\omega^2)} \, d\omega \tag{61}$$

where

$$\beta = t - \frac{x}{U_0}$$

Start with the 1st order Butterworth filter integral

$$I_1 = \frac{1}{\pi} \int_{-\infty}^{\infty} \frac{\omega_c^2}{\omega^2 + \omega_c^2} \, e^{i(\beta\omega - \alpha\omega^2)} \, d\omega \tag{62}$$

This integral can easily be shown to be equivalent to the time domain convolution

$$I_1 = \frac{\omega_c}{2} e^{-\omega_c|\beta|} * \frac{1}{\sqrt{i\pi\alpha}} e^{i\frac{\beta^2}{4\alpha}}$$

which can be expressed as

$$I_1 = \frac{\omega_c}{2\sqrt{i\pi\alpha}} \int_{-\infty}^{\infty} e^{-\omega_c|\tau|} \, e^{i\frac{(\beta-\tau)^2}{4\alpha}} \, d\tau$$

or

$$I_1 = \frac{\omega_c}{2\sqrt{i\pi\alpha}} \left[\int_0^{\infty} e^{-\omega_c\tau} \, e^{i\frac{(\beta-\tau)^2}{4\alpha}} \, d\tau + \int_0^{\infty} e^{-\omega_c\tau} \, e^{i\frac{(\beta+\tau)^2}{4\alpha}} \, d\tau \right] \tag{63}$$

The first integral in (63) can be rewritten as

$$I_{11} = \int_0^{\infty} e^{\left[\frac{i}{4\alpha}\tau^2 - \left(\frac{i\beta}{2\alpha} + \omega_c\right)\tau + \frac{i\beta^2}{4\alpha}\right]} d\tau \tag{64}$$

19

Using relationships in Abromowitz and Stegun (1964), equation (64) has a solution

$$I_{11} = \sqrt{i\pi\alpha}\; e^{\left[i\frac{\beta^2}{4\alpha} + i\left(\sqrt{\alpha}\omega_c + \frac{i\beta}{2\sqrt{\alpha}}\right)^2\right]} erfc\left[\sqrt{i}\left(\sqrt{\alpha}\omega_c + \frac{i\beta}{2\sqrt{\alpha}}\right)\right] \qquad (65)$$

where *erfc* is the complementary error function (1 - *erf*).

Following the same analysis for the second integral in (63) results in

$$I_{12} = \sqrt{i\pi\alpha}\; e^{\left[i\frac{\beta^2}{4\alpha} + i\left(\sqrt{\alpha}\omega_c - \frac{i\beta}{2\sqrt{\alpha}}\right)^2\right]} erfc\left[\sqrt{i}\left(\sqrt{\alpha}\omega_c - \frac{i\beta}{2\sqrt{\alpha}}\right)\right] \qquad (66)$$

Adding (65) and (66) and substituting back into (63) gives, after rearranging and grouping terms

$$I_1 = \frac{\omega_c}{2} e^{i\frac{\beta^2}{4\alpha}}\left[e^{\Psi_1^2(+\beta)} erfc(\Psi_1(+\beta)) + e^{\Psi_1^2(-\beta)} erfc(\Psi_1(-\beta))\right] \qquad (67)$$

where

$$\Psi_1(\pm\beta) = e^{i\frac{\pi}{4}}\left(\sqrt{\alpha}\omega_c \pm i\frac{\beta}{2\sqrt{\alpha}}\right)$$

Equation (67) is the solution to the 1st order Butterworth integral (62). To solve for the nth order Butterworth integral, expand out the Butterworth integrand in equation (61) as partial fractions:

$$\frac{\omega_c^{2n}}{\omega^{2n} + \omega_c^{2n}} = \frac{1}{n}\sum_{k=1}^{n}\frac{\varepsilon_k^2}{\omega^2 + \varepsilon_k^2} \qquad (68)$$

where

$$\varepsilon_k = \omega_c e^{i\theta_k}$$

and

$$\theta_k = \frac{\pi(2k - n - 1)}{2n}$$

Substitute (68) into (61) for

$$I_n = \frac{1}{n}\sum_{k=1}^{n}\frac{1}{\pi}\int_{-\infty}^{\infty}\frac{\varepsilon_k^2}{\omega^2 + \varepsilon_k^2}e^{i(\beta\omega - \alpha\omega^2)}d\omega \qquad (69)$$

The integral in (69) is now equivalent to the 1st order Butterworth integral in (62) which has the solution (67). Substituting (67) into equation (69) gives the final result:

$$I_n = \frac{e^{i\frac{\beta^2}{4\alpha}}}{2n}\sum_{k=1}^{n}\varepsilon_k\left[e^{\Psi_k^2(+\beta)}erfc(\Psi_k(+\beta)) + e^{\Psi_k^2(-\beta)}erfc(\Psi_k(-\beta))\right] \qquad (70)$$

where

$$\Psi_k(\pm\beta) = e^{i\frac{\pi}{4}}\left(\sqrt{\alpha}\varepsilon_k \pm i\frac{\beta}{2\sqrt{\alpha}}\right)$$

$$\varepsilon_k = \omega_c e^{i\theta_k}$$

$$\theta_k = \frac{\pi(2k - n - 1)}{2n}$$

(This page intentionally left blank.)

Appendix B

Digital Butterworth Filters

Software for constructing digital Butterworth filters is both widely available and simple to construct in terms of recursive infinite impulse response (IIR) filters. Kanasewich (1975) and many others discuss the construction of these filters in detail, and it is assumed that the reader is familiar with these algorithms. However, for constructing narrow band-pass filters, it is important to point out several issues in transforming continuous frequency domain filters into equivalent discrete digital time domain filters that can affect this study. To accomplish this, a review of the basic steps involved in Butterworth digital filter construction is appropriate.

B.1 Low-pass Filter Design

a. Start with the square of the transfer function for a low-pass filter (see equation 7):

$$H_L = \frac{1}{1 + \left(\dfrac{\omega}{\omega_c}\right)^{2n}} \tag{71}$$

It is usually assumed that the square root of (71) represents the amplitude spectrum for a causal one-way Butterworth filter. However, for this study, only zero-phase non-causal filters are assumed, realized by applying a causal filter and then the conjugate reverse phase filter, so (71) represents the actual amplitude spectrum for the zero-phase filter.

b. Transform the filter into the Laplace domain with the variable substitution:

$$s = i\frac{\omega}{\omega_c} \quad \rightarrow \quad H_L = \frac{1}{1 + (-1)^n s^{2n}} \tag{72}$$

c. Since (72) is a real function, it can be factored into a polynomial with its conjugate. The polynomial with roots on the left side of the complex plane can be used to construct a stable, causal digital filter:

$$H_L = \frac{1}{B(s)B^*(s)} \quad \rightarrow \quad H_{L1} = \frac{1}{B(s)} \tag{73}$$

d. To transform H_{L1} into a digital filter, use the bilinear z transform for a digital sampling interval dt:

$$s = \frac{2}{dt}\frac{1-z}{1+z} \qquad z = e^{-sdt} \tag{74}$$

e. Substitute (74) into (73) for an equivalent digital filter

$$H_{L(z)} = \frac{\sum_{k=0}^{n} b_k z^k}{1 + \sum_{k=1}^{n} a_k z^k} \qquad (75)$$

Since z is just the Laplacian time shift operator, (75) can easily be set up as a recursive filter for an input signal $X(z)$ as:

$$\left(1 + \sum_{k=1}^{n} a_k z^k\right) Y(z) = \left(\sum_{k=0}^{n} b_k z^k\right) X(z) \qquad (76)$$

f.   To run the filter, transform (76) into the time domain, set initial conditions, and then update $y(t)$ with past values as a recursive filter.

g.   Finally, to run a zero-phase filter, reverse the filtered output $y(t)$ into $x(t)$, rerun (76), and then reverse the filtered output $y(z)$ again. Again, notice that this will have a Butterworth filter amplitude spectrum given by (1).

For brevity, the above review is very condensed, and does not include methods to prewarp the Butterworth cutoff frequency ω_c to account for non-linearity in the bilinear z transform; and methods to cascade the Laplace filter into smaller polynomials to provide more stable time domain filters. See Kanasewich (1975) for details.

B.2 Band-pass Filter Design

The standard approach to constructing a band-pass digital filter is similar to the steps for the low-pass design, except for step b, where a Laplace transform is substituted which maps a band-pass filter with corners ω_1 and ω_2 into a normalized low-pass filter.

a.   The transform that maps the band-pass into low-pass is

$$i\frac{\omega}{\omega_c} = \frac{s^2 + \omega_1 \omega_2}{s(\omega_1 - \omega_2)} \qquad (77)$$

b.   Substituting (77) into (71) gives:

$$H_B = \frac{1}{1 + (-1)^n \left(\dfrac{s^2 + \omega_1 \omega_2}{s(\omega_1 - \omega_2)}\right)^{2n}} \qquad (78)$$

c.   Follow steps c through g under the low-pass design to realize the digital band-pass filter. Notice from (78) that when factoring the Laplace polynomials into conjugate functions in (73),

there will be a factor of s^{2n} in the numerator for the bandpass design. Again, see Kanasewich (1975) for detailed steps in constructing the digital filter.

B.3 Issues

One of the problems in using (78) in the construction of narrow-band time domain recursive filters is the size of the Laplace polynomial. From (78) it can be seen that the maximum order of the polynomial in the denominator will be s^{4n} instead of s^{2n} as in the low-pass case. Although some stability can be gained by cascading filters down to order 2, numerical instability can be a significant issue when using single precision processing with very narrow band-pass filters, when the filters are transformed into recursive form via (74) and (75). *It is essential that computer routines that design and execute recursive band-pass filters with a basic form given by (78) be double precision for all floating-point operators. In addition, for long period calculations (>10 sec) it may be necessary to decimate the time series to 4 samples/sec or less to ensure stability.*

Another issue in using (78) is the non-linearity in transforming a symmetric band-pass filter of the form given by (6) into the modified form (78). Recall that the original band-pass filter (6) was transformed into a low-pass filter by a simple shift in the frequency domain equation (4). Equation (6) is

$$H_1(\omega) = \frac{1}{1 + \left(\dfrac{\omega - \omega_0}{\omega_c}\right)^{2n}} \qquad (79)$$

and can clearly be seen as symmetric about ω_0. Now, it can easily be shown that (78) has the following form for its amplitude spectrum. Let $\omega_1 = \omega_0 - \omega_c$, and $\omega_2 = \omega_0 + \omega_c$. Then

$$H_2(\omega) = \frac{1}{1 + \left(\dfrac{\omega^2 - \omega_1\omega_2}{\omega(\omega_2 - \omega_1)}\right)^{2n}} \qquad (80)$$

It is not obvious, but it can be demonstrated that H_2 is symmetric in log-frequency.

For applications in this report, it is instructive to plot (79) and (80) in a worst case scenario, when the Butterworth cutoff frequency f_c has the maximum width and T is at the shortest period (5 seconds). Assume a 3rd order Butterworth, and let $f_0 = 0.2$ Hz, $f_c = 0.085$ Hz. Plotting in linear and log frequency gives:

25

Amplitude Spectrum - Linear Frequency

Amplitude Spectrum - Log Frequency
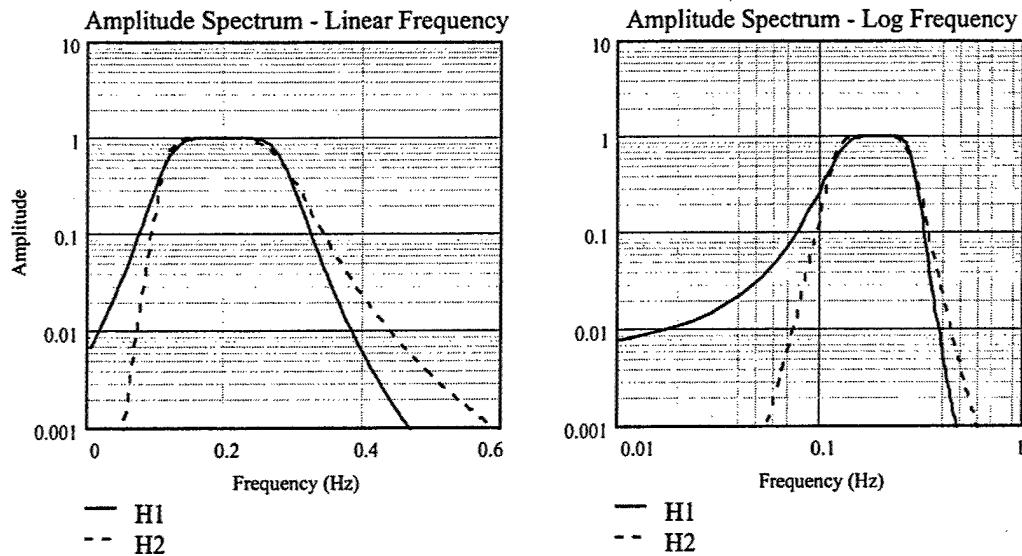
Figure B-1.

From Figure B-1, it would appear that there is a significant effect due to how the band-pass filter is constructed; however, this is only pronounced due to expanding small changes with the logarithmic scale on the amplitude axis. Fast Fourier transforming the above frequency filters into the time domain to give the impulse response show that for purposes of measuring magnitudes, the above effects cause only 2nd order changes in the time domain:

Impulse Response
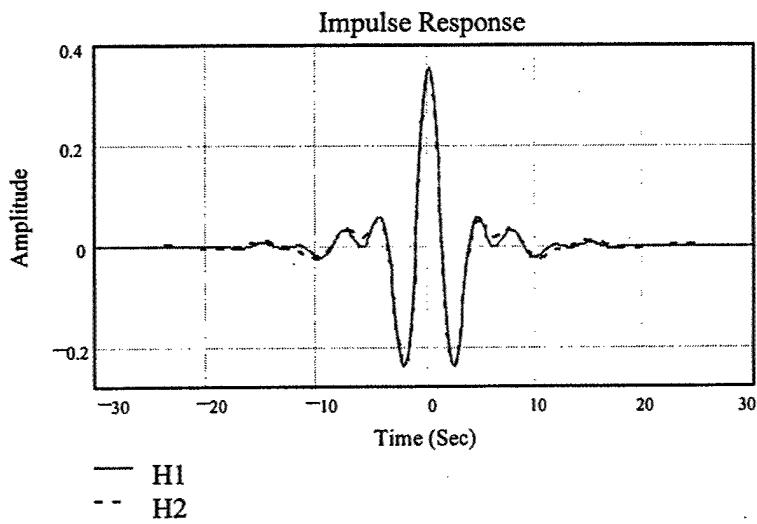
Figure B-2.

Again, the above is the worst-case scenario. As the period increases and the filter width decreases, it can be shown that the difference between H_1 and H_2 decreases. In addition, running synthetic seismograms with both source excitation and attenuation built in show less than .01 magnitude difference when filtered with H_1 and H_2.

B.4 Alternative Time Domain Recursive Filter

As an alternative to the standard IIR design given above, a different transformation can be used to design a recursive narrow-band filter which has the following advantages for operational processing:

- The filter response is equivalent to (79), following the exact theory in this report.

- The filter is built as cascaded first order filters instead of quadratic filters, thus improving the precision for very narrow-band applications.

- The filter returns a *complex* time domain response, which can be used to extract the real filtered response and its envelope function without resorting to Fast Fourier transforms.

- The algorithm has been successfully tested for narrow-band applications in this report, for periods between 5 and 40 seconds, and sampling rates up to 40 samples/second, without requiring decimation.

The basic steps to construct the filter are:

a. Transform the low-pass into band-pass as:

$$p = i\frac{\omega}{\omega_c} = \frac{s - i\omega_0}{\omega_c} \tag{81}$$

or equivalently

$$s = p\omega_c + i\omega_0 \tag{82}$$

This formula represents a simple translation of a low-pass filter from the origin to ω_0, resulting in a complex band-pass filter. Note that this is similar to using the positive half of the Fourier spectrum to form a complex time series, in order to calculate the Hilbert transform for the time series envelope function (Papoulis, page 124, 1962).

b. Substitute (81) into (71) for

$$H_B \quad \rightarrow \quad \frac{1}{1 + (-1)^n (p)^{2n}} \quad \rightarrow \quad \frac{1}{1 + (-1)^n \left(\dfrac{s - i\omega_0}{\omega_c}\right)^{2n}} \tag{83}$$

c. Equation (83) can be factored into poles by first finding the poles p_j for the prototype low-pass filter in (83) (Kanasewich, page 181, 1975) and then substituting these poles into equivalent band-pass poles in (82), resulting in the form

$$H_B = \frac{\omega_c^{2n}}{\prod_{j=1}^{n}(s-s_j)}, \qquad s_j = p_j \omega_c + i \omega_0 \qquad (84)$$

d. Equation (84) can then be cascaded into simple first order filters

$$H_{Bj} = \frac{\omega_c}{s-s_j} \qquad (85)$$

which can be transformed into time domain recursive filters of the form (76) using the bilinear z-transform (74).

e. Finally, after successively running the cascade recursive filters and then reversing for zero phase, the real part of the *complex* time series can be extracted for the narrow-band filtered signal, and the modulus of the series can be calculated for the envelope function.

B.5 Alternative Recursive Filter Coding Algorithm

To realize the above filter, a simple algorithm can be constructed which can be easily coded into C or FORTRAN code:

- Define the following variables and vectors

INTEGER:
m = Butterworth order
n = number of time series points
j,k = counters

REAL
dt = sampling interval
ω_0 = Butterworth band-pass center frequency ($2\pi f_0$)
ω_c = Butterworth band-pass corner frequency ($2\pi f_c$)
$xr(n)$ = input unfiltered time series
$yr(n)$ = output filtered time series
$er(n)$ = output envelope time series
$ermx$ = maximum value of envelope series

COMPLEX DOUBLE PRECISION
$p(m)$ = prototype low-pass Butterworth poles
$s(m)$ = equivalent band-pass Butterworth poles
$a1(m)$ = Z-transform recursive coefficients
$a2(m)$ = Z-transform recursive coefficients
$z1(n)$ = complex time series
$z2(n)$ = complex time series

- Calculate complex poles of Butterworth polynomial

$$p_j = \exp\left[\frac{i\pi}{2m}(2j-1+m)\right] \qquad j = 1,2...m$$

$$s_j = p_j \omega_c + i\omega_0$$

- Calculate complex bilinear z-transform recursive coefficients

$$a1_j = \frac{\omega_c dt}{2 - s_j dt} \qquad j = 1,2...m$$

$$a2_j = \frac{2 + s_j dt}{2 - s_j dt}$$

- Place input time series xr into real part of $z1$

$$z1_k = xr_k \qquad k = 1,2...n$$

- Calculate m cascaded first order filters

$$j = 1,2...m \; ;$$
$$z2_k = z1_k \qquad k = 1,2...n$$
$$z1_1 = a1_j z2_1$$
$$z1_k = a1_j(z2_k + z2_{k-1}) + a2_j z1_{k-1} \qquad k = 2,3...n$$

- Reverse complex time series

$$z2_k = z1_{n-k+1} \qquad k = 1,2...n$$

- Calculate m reversed first order filters ($a1^*, a2^*$ complex conjugates of $a1, a2$)

$$j = 1,2...m \; ;$$
$$z1_k = z2_k \qquad k = 1,2...n$$
$$z2_1 = a1_j^* z1_1$$
$$z2_k = a1_j^*(z1_k + z1_{k-1}) + a2_j^* z2_{k-1} \qquad k = 2,3...n$$

- Reverse complex time series

$$z1_k = z2_{n-k+1} \qquad k = 1,2...n$$

- Calculate output real time series, envelope, and envelope maximum

$$yr_k = 2\,REAL(z1_k) \qquad\qquad k = 1,2...n$$
$$er_k = 2|z1_k|$$
$$ermx = MAX(er_k, ermx)$$

NOTE: For applications given in this report, *bilinear z-transform pre-warping* (Kanasewich, page 192, 1979) *is not required for the above recursive algorithm,* due to the low-pass filter being designed well below the Nyquist frequency.

References

Abromowitz, M., and I. Stegun (1964). *Handbook of Mathematical Functions with Formulas, Graphs, and Mathematical Tables,* U.S. Government Printing Office, Washington, D.C.

Bonner, J.L., D.T. Reiter, and D. Harkrider (2004). *Development of a Time-Domain, Variable-Period Surface Wave Magnitude Measurement Procedure for Application at Regional Distances,* Proceedings of the 26th Annual Seismic Research Review Meeting, Orlando, Florida.

Gutenberg, B. (1945). Amplitudes of surface waves and magnitudes of shallow earthquakes, *Bull. Seism. Soc. Am.* **35,** 3-12.

Herrin, E. and T. Goforth (1977). Phase-matched filters: Application to the study of Rayleigh waves, *Bull. Seism. Soc. Am.* **67,** 1259-1275.

Herrmann, R.B. (1973). Some aspects of band-pass filtering of surface waves, *Bull. Seism. Soc. Am.* **63,** 663-671.

Herrmann, R.B., and B.J. Mitchell (1975). Statistical analysis and interpretation of surface wave anelastic attenuation data for the stable interior of North America, *Bull. Seism. Soc. Am.* **65,** 1115-1128.

Kanamori, H., and G.S. Stewart (1976). Mode of strain release along the Gibbs Fracture Zone, Mid-Atlantic Ridge, *Phys. Earth Planet. Inter.,* 11, 312-332.

Kanasewich, E.R. (1975). *Time Sequence Analysis in Geophysics,* University of Alberta Press, Edmonton, Alberta, Canada, p. 179.

Marshall, P.D., and P.W. Basham (1972). Discrimination between earthquakes and underground explosions employing an improved M_s scale, Geo*phys. J. R. Astr. Soc.,* **29,** 431-458.

Mathews, J., and R.L. Walker, (1970). *Mathematical Methods of Physics,* Benjamin/Cummings Publishing Co., Menlo Park, Ca.

Okal, E.A., (1989). A theoretical discussion of time domain magnitudes: the Prague formula for M_s and the mantle magnitude M_m, *J. Geophys. Res.* **94,** 4194-4204.

Papoulis, A. (1962). *The Fourier Integral and Its Applications,* McGraw-Hill, New York.

Rezapour, M., and Pearce, R.G. (1998). Bias in surface-wave magnitude M_s due to inadequate distance corrections, *Bull. Seism. Soc. Am.* **88,** 43-61.

Richards, P.G., and K. Aki (1980). *Quantitative Seismology: Theory and Methods,* W. H. Freeman and Co., San Francisco, p. 266.

Vaněk, J., A. Zatopek, V. Karnik, N.V. Kondorskaya, Y.V. Riznichenko, E.F. Savarensky, S.L. Solov'ev, and N.V. Shebalin (1962). Standardization of magnitude scales, *Bull. Acad. Sci. USSR, Geophys. Ser.,* no. 2, 108-111 (English Translation).

von Seggern, D.H. (1977). Amplitude-distance relation for 20-second Rayleigh waves, *Bull. Seism. Soc. Am.* **67,** 405-411.

Yacoub, N.K. (1983). "Instantaneous Amplitudes": a new method to measure seismic magnitude, *Bull. Seism. Soc. Am.* **73,** 1345-1355

Distribution

California Institute of Technology
ATTN: Prof. Thomas Ahrens
Seismological Laboratory, 252-21
Pasadena CA 91125

Air Force Research Laboratory/VSBL
ATTN: Mr. R. Raistrick & Dr. A. Dainty
29 Randolph Rd.
Hanscom AFB MA 01731-3010

DATSD(CD&TR)
ATTN: Mr. Patrick Wakefield
1515 Wilson Blvd., Suite 720
Arlington VA 22209

Pennsylvania State University
ATTN: Prof. S. Alexander & Prof. C. Langston
Department of Geosciences
537 Deike Building
University Park PA 16802

University of Colorado
ATTN: Prof. C. Archambeau, Prof. D. Harvey,
     Dr. Anatoli Levshin, & Prof. M. Ritzwoller
Department of Physics/JSPC
3100 Marine Street
Boulder CO 80309-0583

Cornell University
ATTN: Prof. M. Barazangi
Institute for the Study of the Continents
Department of Geological Sciences
3126 SNEE Hall
Ithaca NY 14853

State University of New York, Binghamton
ATTN: Prof. F.T. Wu
Department of Geological Sciences
Binghamton NY 13901

ENSCO, Inc./APA Division
ATTN: Dr. D.R. Baumgardt & Dr. Z. Der
5400 Port Royal Road
Springfield VA 22151-2388

University of Arizona
ATTN: Dr. S. Beck
Department of Geosciences
Gould Simpson Building
Tucson AZ 85721

University of California, San Diego
ATTN: Dr. J. Berger, Dr. F.L. Vernon,
     Dr. M. Hedlin, & Prof. B. Minster,
Scripps Institution of Oceanography
Institute of Geophysics and Planetary Physics
9500 Gilman Dr., IGPP, A-025
La Jolla CA 92093

University of California, San Diego
ATTN: Dr. John Orcutt
Director's Office (0210)
Scripps Institution of Oceanography
La Jolla CA 92093-0225

US Department of Energy
ATTN: Ms. Leslie A. Casey
NNSA/NA-22
1000 Independence Ave., SW
Washington DC 20585-0420

Multimax, Inc.
ATTN: Dr. W. Chan, Dr. I.N. Gupta,
     & Mr. W. Rivers
1441 McCormick Drive
Largo MD 20774

Virginia Polytechnical Institute
ATTN: Dr. M. Chapman
Seismological Observatory
Department of Geological Sciences
4044 Derring Hall
Blacksburg VA 24061-0420

US Department of State
AC/VC
ATTN: Dr. C. Yeaw & Mr. R. Morrow
2201 C Street, N.W.
Washington DC 20520

US Geological Survey
ATTN: Dr. William Leith
National Center, MS-951
12201 Sunrise Valley Dr.
Reston VA 20192

University of Connecticut, Storrs
ATTN: Prof. V.F. Cormier
Department of Geology & Geophysics
U-45, Room 207
Storrs CT 06269-2045

DTRA/TDAS
ATTN: Dr. R.A. Gustafson
8725 John J. Kingman Rd., MS6201
Ft. Belvoir VA 22060

University of California, San Diego
ATTN: Dr. Catherine de Groot-Hedlin
Institute of Geophysics & Planetary Sciences
8604 La Jolla Shores Drive
San Diego CA 92093

Harvard University
ATTN: Prof. A. Dziewonski
Hoffman Laboratory
Department of Earth, Atmospheric & Planetary
    Sciences
20 Oxford Street
Cambridge MA 02138

Boston College
ATTN: Prof. J. Ebel & Prof. A. Kafka
Department of Geology & Geophysics
Chestnut Hill MA 02167

Mission Research Corporation
ATTN: Dr. M. Fisk
8560 Cinderbed Rd., Suite 700
Newington VA 22122

Southern Methodist University
ATTN: Dr. Henry Gray
Department of Statistical Science
P.O. Box 750302
Dallas TX 75275-0302

Pacific Northwest National Laboratories
ATTN: Dr. D.N. Hagedorn
P.O. Box 999, MS K5-12
Richland WA 99352

Lawrence Livermore National Laboratory
ATTN: Dr. J. Zucca
P.O. Box 808, L-175
Livermore CA 94551

Dr. David Harkrider
24 Martha's Point Rd.
Concord MA 01742-4917

New Mexico State University
ATTN: Prof. Thomas Hearn & Prof. James Ni
Department of Physics, 3D
Las Cruces NM 88003

California Institute of Technology
ATTN: Dr. Donald Helmberger
Division of Geological & Planetary Sciences
Seismological Laboratory
Pasadena CA 91125

Southern Methodist University
ATTN: Dr. E. Herrin & Dr. B. Stump
Department of Geological Sciences
P.O. Box 750395
Dallas TX 75275-0395

Sandia National Laboratories
ATTN: Mr. Pres Herrington
P.O. Box 5800, MS 0572
Albuquerque NM 87185-0572

St. Louis University
ATTN: Prof. R. Herrmann & Prof. B. Mitchell
Department of Earth & Atmospheric Sciences
3507 Laclede Ave.
St. Louis MO 63103

AFTAC/CA(STINFO)/TT/TTD/TTE/TTR
1030 South Highway A1A
Patrick AFB FL 32925-3002

University of California, Berkeley
ATTN: Prof. L.R. Johnson
Earth Sciences Division
LBNL 90-2106, MS 90-1116
479 McCone Hall
Berkeley CA 94720

Massachusetts Institute of Technology
ATTN: Prof. T.H. Jordan
Department of Earth, Atmospheric, & Planetary
   Sciences
77 Massachusetts Ave., 654-918
Cambridge MA 02139

Massachusetts Institute of Technology
ATTN: Dr. R. LaCross, M-200B
Lincoln Laboratory
P.O. Box 73
Lexington MA 02173-0073

University of Illinois, Urbana-Champaign
ATTN: Prof. F.K. Lamb & Prof. J. Sullivan
Department of Physics
1110 West Green Street
Urbana IL 61801

Oklahoma Geological Survey Observatory
ATTN: Dr. J. Lawson, Chief Geophysicist
Number One Observatory Lane
P.O. Box 8
Leonard OK 74043-0008

University of California, Santa Cruz
ATTN: Dr. T. Lay, Dr. S. Schwartz, & Dr. R. Wu
Institute of Tectonics, Earth Sciences Dept.
1156 High St., A232
Santa Cruz CA 95064

US Geological Survey
ATTN: Dr. John Filson
12201 Sunrise Valley Dr., MS-905
Reston VA 20192

Weston Geophysical Corp.
ATTN: Mr. James Lewkowicz
57 Bedford St., Ste 102
Lexington MA 02420

Georgia Institute of Technology
ATTN: Prof. L. Long
School of Geophysical Sciences
Atlanta GA 30332

Southern Methodist University
ATTN: Dr. G. McCartor
Department of Physics
P.O. Box 750175
Dallas TX 75275-0175

US Geological Survey
ATTN: Dr. A. McGarr
National Earthquake Center
345 Middlefield Rd., MS-977
Menlo Park CA 94025

Office of the Secretary of Defense
DDR&E
Washington DC 20330

Yale University
ATTN: Prof. J. Park
Department of Geology & Geophysics
P.O. Box 208109
New Haven CT 06520-8109

University of Cambridge
ATTN: Prof. Keith Priestly
Bullard Lab, Department of Earth Sciences
Madingley Rise, Madingley Road
Cambridge CB3 OEZ
UNITED KINGDOM

BBN Systems & Technologies
ATTN: Dr. J.J. Pulli
1300 N. 17th St., Suite 1200
Arlington VA 22209

Weston Geophysical Corp.
ATTN: Dr. Delaine Reiter
57 Beford St., Ste 102
Bedford MA 02420

Columbia University
ATTN: Prof. P. Richards & Dr. J. Xie
Lamont-Doherty Earth Observatory
61 Route 9W
Palisades NY 10964

Woodward-Clyde Federal Services
ATTN: Dr. C.K. Saikia
566 El Dorado Street, Suite 100
Pasadena CA 91101-2560

University of Southern California, Los Angeles
ATTN: Prof. C.G. Sammis
Department of Earth Sciences
University Park
Los Angeles CA 90089

Secretary of the Air Force
(SAFRD)
Washington DC 20330

University of California, Davis
ATTN: Dr. R. Shumway
Division of Statistics
1 Shields Ave.
Davis CA 95616-8671

AFOSR/NL
110 Duncan Avenue, Suite B115
Bolling AFB
Washington DC 20332-0001

Los Alamos National Laboratory
ATTN: Dr. H. Patton, Dr. S.R. Taylor,
    Dr. C.L. Edwards, Dr. D.C. Pearson,
    Dr. Scott Phillips, & Dr. T. Wallace
P.O. Box 1663, MS D408
Los Alamos NM 87545

Massachusetts Institute of Technology
ATTN: Prof. M.N. Toksoz
Earth Resources Lab, 34-440
42 Carleton Street
Cambridge MA 02142

WINPAC/CA/FO
ATTN: Dr. L. Turnbull
New Headquarters Bldg., Room 4W03
Washington DC 20505

National Science Foundation
ATTN: Dr. Daniel Weill
Division of Earth Sciences, EAR-785
4201 Wilson Blvd., Room 785
Arlington VA 22230

NTNF/NORSAR
ATTN: Dr. Svein Mykkeltveit
P.O. Box 53
N-2007 Kjeller
NORWAY

Geoscience Australia
Australian Geological Survey Organization
ATTN: Dr. David Jepsen
GPO Box 378
Canberra City, ACT 2601
AUSTRALIA

Atomic Weapons Establishment Blacknest
ATTN: Dr. David Bowers & Dr. Alan Douglas
Brimpton, Nr Reading
Berkshire RG7 4RS
UNITED KINGDOM

University of Bergen
ATTN: Prof. Eystein Husebye
Institute for Solid Earth Physics, IFJ
Allegaten 41
N-5007, Bergen
NORWAY